J Solid State Electrochem (2010) 14:981–988
DOI 10.1007/s10008-009-0897-z

ORIGINAL PAPER

# Mathematical modeling and numerical simulation of metal nanoparticles electrooxidation

**Khiena Z. Brainina · Leonid G. Galperin · Aleksandr L. Galperin**

Received: 30 April 2009 / Revised: 24 June 2009 / Accepted: 25 June 2009 / Published online: 22 July 2009


**Abstract** A mathematical model is proposed that describes the processes of electrooxidation of metal nanoparticles localized on the surface of an indifferent macroelectrode. In contrast to previously proposed models based on geometric factors (shapes of particles and diffusion zones), the proposed model has introduced thermodynamic considerations which take into account the energy differences between the nanoparticle ensembles from microparticles and macroparticles. A series of voltammograms was obtained as a result of calculations and characteristic relationships between the different parameters were found. An analysis of the findings, on the one hand, predicts the shape and characteristic features of the experimental voltammograms and, on the other hand, provides information regarding energetic properties of the nanoparticles.

K. Z. Brainina (✉)
Ural State University of Economics,
8 Marta St, 62,
Yekaterinburg 620219, Russia
e-mail: baz@usue.ru

K. Z. Brainina
Institute of Medical Cell Technologies,
Soboleva St, 25,
Yekaterinburg 620095, Russia

L. G. Galperin
Ural State Technical University – UPI,
Mira st., 19, A-203,
Yekaterinburg 620002, Russia

A. L. Galperin
Ural State University,
Lenin Avenue 51,
Yekaterinburg 620083, Russia

**Keywords** Nanoparticles · Electrooxidation · Mathematical modeling

## Introduction

Nanotechnology has vast potential in developing new constructive material, fuel cells, microreactors, drug delivery and imaging devices, biosensor parts, and personal care products. A number of properties of nanostructural materials (NSM; considerable specific surface and, consequently, high adsorptivity) afford prospects for using NSM to create a new class of chemical and biological sensors. Nanoparticles are used in such sensors as transducers, catalytic components, and markers [1–7].

The development of nanotechnologies and the expanded practical application of nanomaterials require comprehensive information regarding their properties. Electrochemical methods can provide very valuable information both for analysis of the thermodynamic and energy properties, as well as the kinetics of redox reactions, in addition to methods of dynamic light scattering and electron and atomic force microscopy.

The goal of the proposed work is a mathematical modeling of the electrooxidation processes of metal nanoparticles, a search for a representation of the size and surface energy effects in the form of experimental curves, and further study of the sensory properties of nanoparticles in particular.

Some previous studies in this field of research need to be mentioned here: thus, *Compton* and coauthors [8, 9] proposed a mathematical model for the electrochemical stripping of silver or bismuth nanoparticles from a solid electrode. Model is based on geometrical and diffusion approach.

Our aim is to take into account size-dependent energy effects on electrode process, extending approaches given in previous works. It is based on the concept introduced in [10, 11], in which different energetic states of the metal were distinguished as the energy spectrum of the metal: $M_{\mathrm{I}}$ ($\Delta G°<0$), $M_{\mathrm{II}}$ ($\Delta G°=0$), $M_{\mathrm{III}}$ ($\Delta G°>0$),where $M_{\mathrm{I}}$, $M_{\mathrm{II}}$, $M_{\mathrm{III}}$ denotes metal in the first, second, and third energy states, respectively; $\Delta G°$ is Gibbs energy.

It was assumed that in case of the metal $M_{\mathrm{I}}$ (adsorbate, adatoms) the metal is bound to the electrode surface more strongly than in the bulk crystal lattice (metal in the second energy state $M_{\mathrm{II}}$). It corresponds to the minimum energy state of the system metal–electrode. An in-depth discussion of the adatoms on the electrode is outside the scope of this paper. For detailed discussion of adatoms on electrodes, see [10, 11]. $M_{\mathrm{II}}$ corresponds to equilibrium state. $M_{\mathrm{III}}$ is energy-rich state that is typical for the systems, where surface energy should not be omitted from the consideration We propose an approach capable of treating the electrochemical dissolution of nanoparticles when such energetic considerations are crucial.

## Mathematical modeling and numerical simulation

Our model for electrooxidation is based on the following assumptions:

1. The impact of the surface layer on the phase overall properties is determined by the specific surface per unit of volume ($S/V$).
2. Electrooxidation is described by an electrical charge balance equation: $\mathrm{Me} = \mathrm{Me}^{n+} + ne$.
3. Kinetics of the process is determined by:
   (a) The rate of electron transfer
   (b) The diffusion removal of metal ions from the surface
4. On the surface of an electrode with area $S_{\mathrm{e}}$, hereinafter considered to be an infinite plane, initially, there is $Q_0$ a mixture of uniformly distributed spherical nanoparticles with radius $r_{0\ \mathrm{II}}$ (metal in the second state) and $r_{0\ \mathrm{III}}$ (metal in the third state) larger and smaller than a certain critical radius $r_{\mathrm{cr}}$, respectively. The percentage of subcritical size particles in the mixture equals $\delta$. Electrooxidation processes in polydispersional systems will be discussed in a future publication.
5. Change of potential $E$ from its initial value $E_{\mathrm{in}}$ with rate $\nu$ leads to electrodissolution of the particles, observed as a current $i = i_{\mathrm{II}} + i_{\mathrm{III}}$
6. The total quantity of electricity $Q_0$ that might flow during dissolution of all the particles from the surface of an indifferent electrode (initial charge) is $Q_0 = Q_{0\,\mathrm{II}} + Q_{0\,\mathrm{III}}$.
7. Sufficient electrolyte is present to suppress migration effects.
8. The current magnitudes are proportional to the surface area of the corresponding particles.
9. Calculations of the voltamperograms describing nanoparticles electrodissolution from the indifferent electrode surface are based on the following expressions that determine the electrical current magnitude:

$$i = i_{\mathrm{II}} + i_{\mathrm{III}}; \tag{1}$$

$$i_{\mathrm{II}} = n F k_s S_{\mathrm{II}}(t) \left\{ a_M \exp\left[\frac{n\beta F}{RT}\left(E - E^0\right)\right] - c(x=0,\,t)\exp\left[-\frac{n\alpha F}{RT}\left(E - E^0\right)\right]\right\}; \tag{2}$$

$$i_{\mathrm{III}} = n F k_s S_{\mathrm{III}}(t)\left\{ a_M \exp\left[\frac{n\beta F}{RT}\left(E - E^0\right) + \frac{\beta \Delta G^0}{RT}\right] - c(x=0,\,t)\exp\left[-\frac{n\alpha F}{RT}\left(E - E^0\right) - \frac{\alpha \Delta G^0}{RT}\right]\right\}; \tag{3}$$

Here, $x$ is coordinate normal to the surface ($x=0$ corresponds to a point on the plane), $c(x=0,t)$ is concentration of the particles on the electrode surface at time $t$; $i(t)$ is the current. Usually, this concentration ($c(x,t)$) is calculated solving the partial differential equations for a sample particle taking into account the particles distribution on the surface. Alternatively, the concentration $c(t)$ can be determined directly from the current $i(t)$. Taking into account the small diameter of the particles (compared to the dimensions of the electrode), the field of concentrations near the surface can be determined by solving the diffusion problem in which the electrode is viewed as a continually operating flat source of ions. These ions come to the solution while the nanoparticles are being dissolved. This assumption allows avoiding the necessity of the detailed modeling of the dissolution kinetics. Hence, concentration field near the electrode surface depends only on the coordinate normal to the surface.

The solution of a similar problem of heat conductance by the Green function method is given in [12]. The field of concentrations in the vicinity of the electrode in this situation is described by the formula:

$$c(x,\,t) = \frac{1}{\sqrt{4\pi D}} \int_0^t \exp\left\{-\frac{x^2}{4D\,(t-\tau)}\right\} \frac{\phi(\tau)\,\mathrm{d}\tau}{\sqrt{t-\tau}}, \tag{4}$$

Here, $\phi(t)$ is output of the source per unit of surface area per second:

$$\phi(t) = \frac{i}{nF S_e}, \tag{5}$$

Charge balance equations

$$Q_{\mathrm{II}} = Q_{0\mathrm{II}} - \int_0^t i_{\mathrm{II}}\,\mathrm{d}t, \tag{6}$$

$$Q_{\mathrm{III}} = Q_{0\mathrm{III}} - \int_0^t i_{\mathrm{III}}\,\mathrm{d}t \tag{7}$$

close the model.

Here:

$$Q_{0\mathrm{II}} = A\,r_{0\mathrm{II}}^3 = \frac{4}{3}\,\pi\,r_{0\mathrm{II}}^3\,\rho\,\frac{nFN_{\mathrm{II}}}{M}; \tag{8}$$

$$Q_{0_{\mathrm{III}}} = A\,r_{0\mathrm{III}}^3 = \frac{4}{3}\,\pi\,r_{0\mathrm{III}}^3\,\rho\,\frac{nFN_{\mathrm{III}}}{M}; \tag{9}$$

$$Q_{\mathrm{II}} = A\,\xi_{\mathrm{II}}{}^3 = \frac{4}{3}\,\pi\,\xi_{\mathrm{II}}{}^3\,\rho\,\frac{n\,FN_{\mathrm{II}}}{M}; \tag{10}$$

$$Q_{\mathrm{III}} = A\,\xi_{\mathrm{III}}^3 = \frac{4}{3}\,\pi\,\xi_{\mathrm{III}}^3\,\rho\,\frac{n\,FN_{\mathrm{III}}}{M}. \tag{11}$$

Surface of the particles at initial and subsequent times is determined by Eqs. 12 and 13

$$S_{\mathrm{II}}(0) = N_{\mathrm{II}}\,4\,\pi\,r_{0\mathrm{II}}^2; \quad S_{\mathrm{II}}(t) = N_{\mathrm{II}}\,4\,\pi\,\xi_{\mathrm{II}}^2; \tag{12}$$

$$S_{\mathrm{III}}(0) = N_{\mathrm{III}}\,4\,\pi\,r_{0\mathrm{III}}^2; \quad S_{\mathrm{III}}(t) = N_{\mathrm{III}}\,4\,\pi\,\xi_{\mathrm{III}}^2. \tag{13}$$

Here:

$E = E_{\mathrm{in}} + vt$
$k_s$—constant of the electrode process rate, cm $s^{-1}$;
$n$—number of electrons participating in the electrode process;
$F$—Faraday number, C $mol^{-1}$;
$a_{\mathrm{M}}$ —solid-phase activity, mol $cm^{-3}$;
$\alpha$, $\beta$—electrode process transfer coefficients;
$R$—universal gas constant, J $mol^{-1}$ $K^{-1}$;
$T$—temperature, °K;
$E_{\mathrm{in}}$—initial potential, V;
$\nu$—potential scan rate, V $s^{-1;}$
$M$—molecular mass, g $mol^{-1}$;
$\rho$—specific density, g $cm^{-3}$;
$N$—number of particles of each kind

The mathematical model for the oxidation of a two-dimensional set of nanoparticles is thus expressed by Eqs. 1–13. These equations are solved numerically. The calculations employs an explicit scheme with time step $h_1 = 10^{-5}$s (see [12] for detailed discussion). Initial condition is $c(t=0)=0$ and $i(t=0)=0$. The initial magnitudes of total charge and initial radiuses of the dissolved particles are $Q_{0\mathrm{II}}$, $Q_{0\mathrm{III}}$, and $r_{0\mathrm{II}}$, $r_{0\mathrm{II}}$, respectively. At each step $t$, current $i(t)$ is obtained from Eqs. 1–3 using concentration from the previous time step $c(t-h)$. $i(t)$ is then used in Eq. 4 providing concentration $c(t)$.

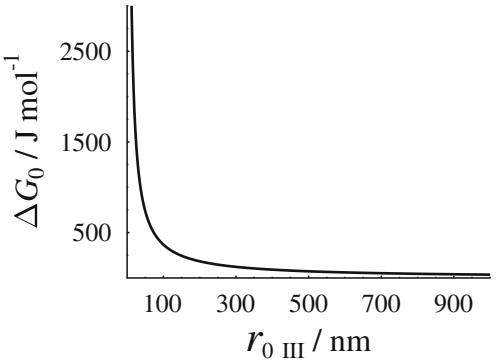


**Fig. 1** Dependence of Gibbs surface energy on particle radius

Comparison of the calculated according to the discussed model voltammograms with the experimental ones will be given in the next paper and will be the evidence of the approach adequacy.

## Numerical results

Analysis of the aforementioned problem shows that almost all the parameters of the model are either tabular quantities or data assigned by the experimental conditions such as temperature, particle size, and amount of substance in the particles (initial charge) and rate of potential sweep. The magnitude of the Gibbs surface energy is an exception and its selection needs to be clarified. Although the latter can be calculated easily:

$$\Delta G^{\circ} = \sigma \times S \tag{14}$$

($\sigma$ is surface tension).

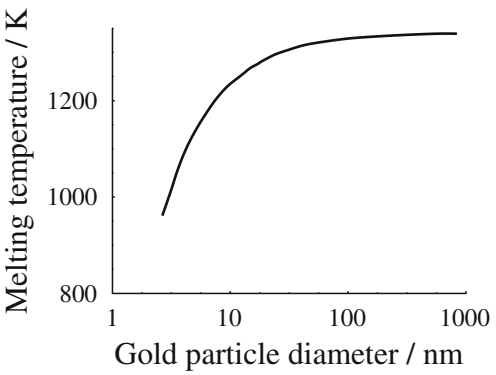


**Fig. 2** Dependence of gold melting point on the particle diameter. Reprinted with permission from Cristina et al. [13]

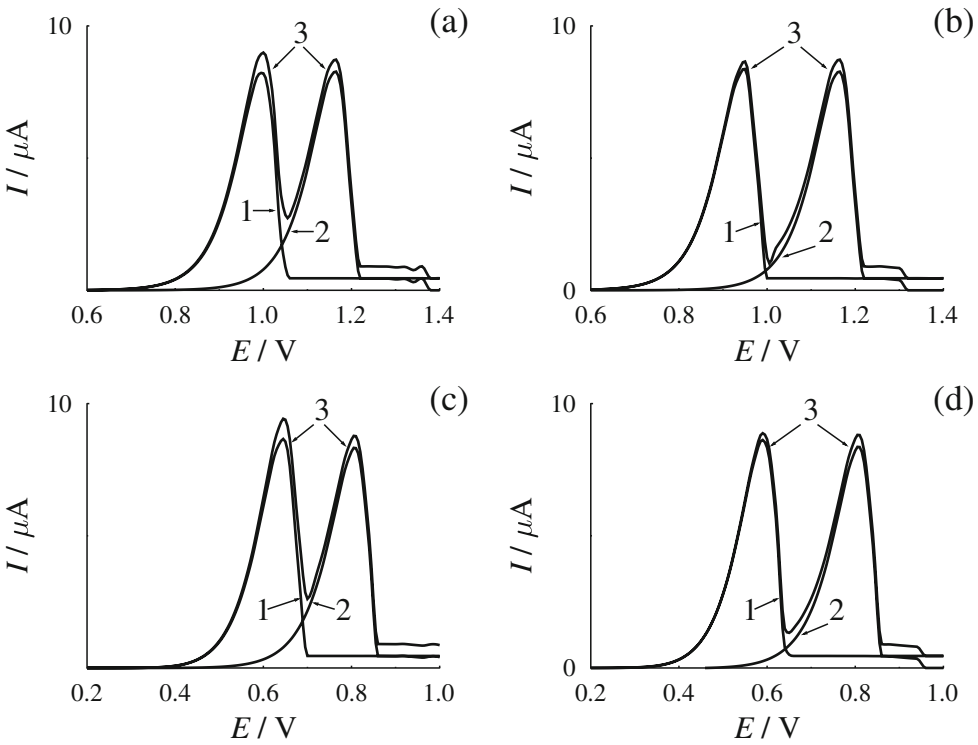


**Fig. 3** Voltammograms calculated using: $M$=196.96 g mol$^{-1}$, $E°$=0.95 V, $\rho$=19.3 g cm$^{-3}$, $v$=0.10 V s$^{-1}$, $E_{in}$= 0.00 V, $\delta$=0.50, $Q_0$=20 μC, $r_{0\ III}$=40 nm, $r_{0\ II}$=1 μm, $k_s$= $10^{-7}$cm s$^{-1}$ (**a**, **b**), and $k_s$=$10^{-4}$ cm s$^{-1}$ (**c**, **d**), $\Delta G°$= 0 (**a**, **c**), and $\Delta G°$= 5,000 J mol$^{-1}$ (**b**, **d**). (*1*) $I_{III}$, (*2*) $I_{II}$, (*3*) $I_{III}+I_{II}$

However, the results of these calculations can hardly yield a precise value for $\Delta G°$ since surface tension on the interface of the solid state–water/air is not always exactly known. Nevertheless, as a certain approximation, the proposed method can be considered reasonable.

Figure 1 shows the calculated dependence of $\Delta G°$ on $r$ (Eq. 14 and correlation between $S$ and $r$ were used). It is apparent from the figure that there is a significant change in the nature of this dependence if the radius is smaller than 100 nm. When the particle radius exceeds 100 nm, the Gibbs energy almost does not depend on the particle radius.

Figure 2 shows dependence of gold melting point on the particle diameter taken from [13]. It is easily discernible that the melting point of particles with diameter greater than 50 nm becomes equal to the melting point of bulk gold; the melting point of particles with diameter less than 50 nm is significantly lower than the melting point of the bulk metal. Similar results were obtained during the study of properties of silicon nanoparticles [14]. It can be concluded from a comparison of data given on the Figs. 1 and 2 that, on the one hand, the particles with diameter over 50–100 nm are close in properties to the bulk metal phase and the sample passes from a state $M_{III}$ to a state $M_{II}$. On the other hand, the correlation of calculated and experimental data indicates the plausibility of the selected method to account for the nanoparticle energy characteristics. Taking these data into account, there is a natural conclusion that the properties of the system consisting of particles with radius equal to or exceeding 1 μm do not differ from the properties of the bulk phase. With the exception of an especially stipulated cases, $r_{II}$=1 μm for the metal particles $M_{II}$ is used for the calculations.

Figure 3 shows voltammograms calculated using $r_{0\ III}$= 40 nm, $r_{0\ II}$=1 μm, $k_s$=$10^{-7}$ and $10^{-4}$cm s$^{-1}$, and $\Delta G°$= 0 and 5,000 J mol$^{-1}$. The impact of $\Delta G°$ increase is expressed as a current shift $I_{III}$ towards current $I_{II}$ and reduction in the difference of the current maximum potentials. It means that the properties of the system are shifted from nano ($M_{III}$) to the bulk metal—($M_{II}$) state. The behavior mentioned is obviously the consequence of Gibbs surface energy impact into the system energy. Electrode process kinetics ($k_s$ increase) is reflected in the shift of potential maximums to less-positive potentials in comparison to the voltammograms for smaller $k_s$.

Figures 4 and 5 show voltammograms that were calculated for particles of varying size with $k_s$=$10^{-7}$ (irreversible process) and $k_s$=$10^{-4}$ (reversible process). It is easy to see that increase in the particle radius results in a conversion of the curve with two separate peaks into a curve with overlapping peaks and then into a voltammogram with one current peak regardless of $k_s$ and the initial quantity of substance $Q_0$ on the electrode surface. The voltammograms describing reversible process are shifted to less-positive potentials in comparison to the voltammograms for irreversible process. Kinetics of the process is reflected in the nature of the dependence of the maximum current on the particle size (Fig. 6). It is apparent that, in the irreversible process, currents $I_{II}$ and $I_{III}$ do not depend on the particle size and essentially do not differ in magnitude (when $Q_{II}$=$Q_{III}$). In the reversible process, current $I_{III}$ increases drastically when the

particle radius becomes smaller 50 nm and $I_{III}>I_{II}$ under conditions when the currents do not differ in the irreversible process (with $Q_{II}=Q_{III}$).

Figure 7 shows the dependence of the difference in potentials of current maximums $\Delta E_{max} = E_{max(II)} - E_{max(III)}$ on $\Delta G°$, calculated for particles of varying size (a), and on particle radius, calculated for different $\Delta G°$ (b).

An increase is observed in the difference of current peak potentials with an increase in $\Delta G°$ and decrease when the particle radius rises. However, the $\Delta E_{max}=f(\Delta G°)$ plot is not extrapolated to zero. The difference in $\Delta E_{max}$ from zero is greater as the particle radius becomes smaller. In addition to this energy factor ($\Delta G°$), during electrooxidation of nano-

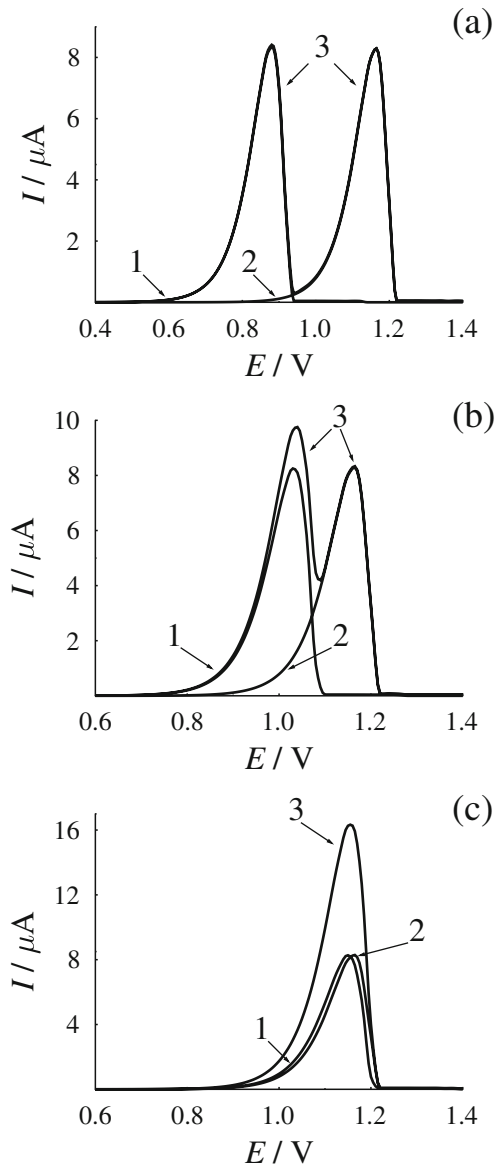


**Fig. 4** Voltammograms calculated for varying size particles with $\Delta G°=1{,}000$ J mol$^{-1}$, $k_s=10^{-7}$cm s$^{-1}$, $Q_0=20$ μC, $r_{0\ III}=5$ (**a**), 100 nm (**b**), 1 μm (**c**); $r_{0\ II}=1$ μm. (*1*) $I_{III}$, (*2*) $I_{II}$, (*3*) $I_{III}+I_{II}$. Other parameters are given in the Fig. 3 caption

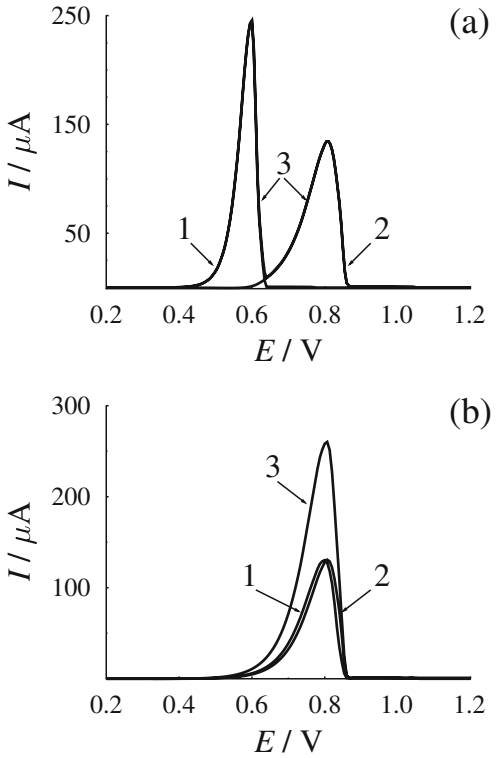


**Fig. 5** Voltammograms calculated for $k_s=10^{-4}$cm s$^{-1}$, $\Delta G°=1{,}000$ J mol$^{-1}$, $Q_0=300$ μC, $r_{0\ III}=5$ nm (**a**) and 1 μm (**b**). (*1*) $I_{III}$, (*2*) $I_{II}$, (*3*) $I_{III}+I_{II}$. Other parameters are given in the Fig. 3 capture

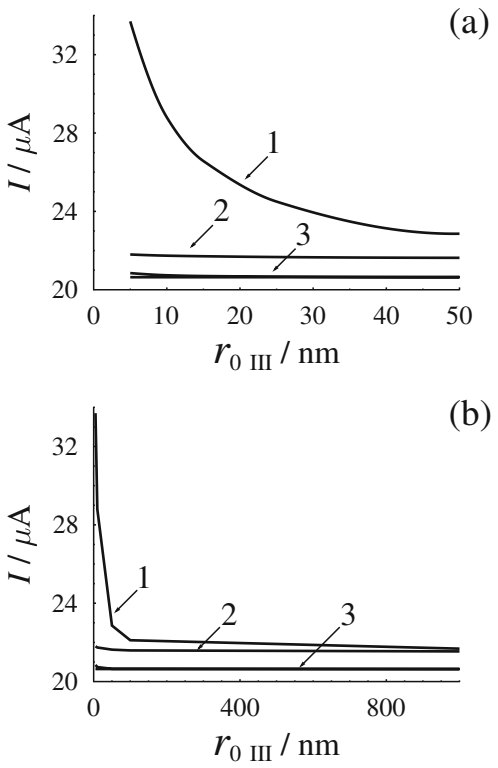


**Fig. 6** **a**, **b** Maximal current dependence on the particle radius calculated for $Q_0=50$ μC, $\Delta G°=1{,}000$ J mol$^{-1}$, $k_s=10^{-4}$cm s$^{-1}$ (*1*, *2*) and $k_s=10^{-7}$cm s$^{-1}$ (*3*), (*1*) $I_{III}$, (*2*) $I_{II}$, (*3*) $I_{III}$, $I_{II}$. Other parameters are given in the Fig. 3 caption

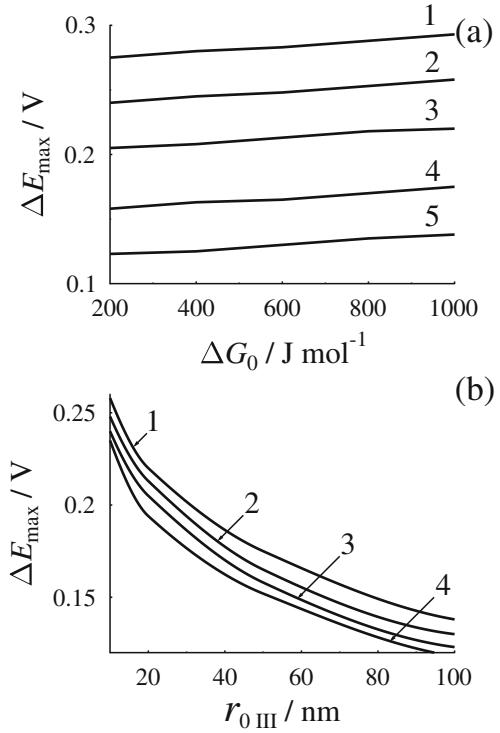


**Fig. 7** Dependence of maximal current potential difference $\Delta E_{max}=E_{max}(I_{II})-E_{max}(I_{III})$ on $\Delta G°$, calculated for the varying size particles (**a**) and on particle radius for the different $\Delta G°$ (**b**): $k_s=10^{-7}$cm s$^{-1}$, $Q_0=20$ μC, $r_{0III}=5$, 10, 20, 50, 100 nm (**a**), $\Delta G°=1{,}000$, 600, 200, 0 J mol$^{-1}$ (**b**). Other parameters are given in the Fig. 3 caption

particles, the geometric component evidently contributed. We note that the kinetics of the process has little impact on the dependence of $\Delta E_{max}$ on $\Delta G°$ and particle radius. The corresponding curves calculated for reversible and irreversible processes ($k_s=10^{-4}$ and $10^{-7}$) differ only for very small particles (Fig. 8).

Figure 9 represents voltammograms calculated for reversible ($k_s=10^{-4}$) electrooxidation of nanoparticles, the size of which slightly differs. At $\Delta G°=0$ currents $I_{II}$ and $I_{III}$

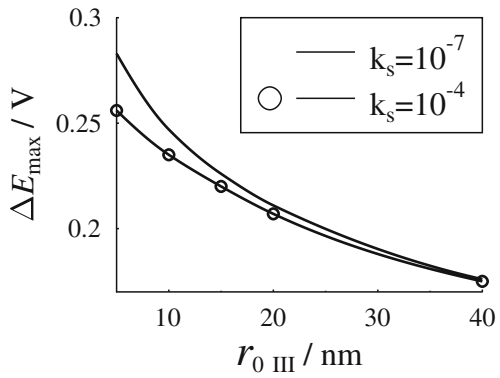


**Fig. 8** Dependence of maximal current potential difference $\Delta E_{max}=E_{max}(I_{II})-E_{max}(I_{III})$ on particle radius, calculated for $\Delta G°=1{,}000$ J mol$^{-1}$, $Q_0=20$ μC and different $k_s$. Other parameters are given in the Fig. 3 caption

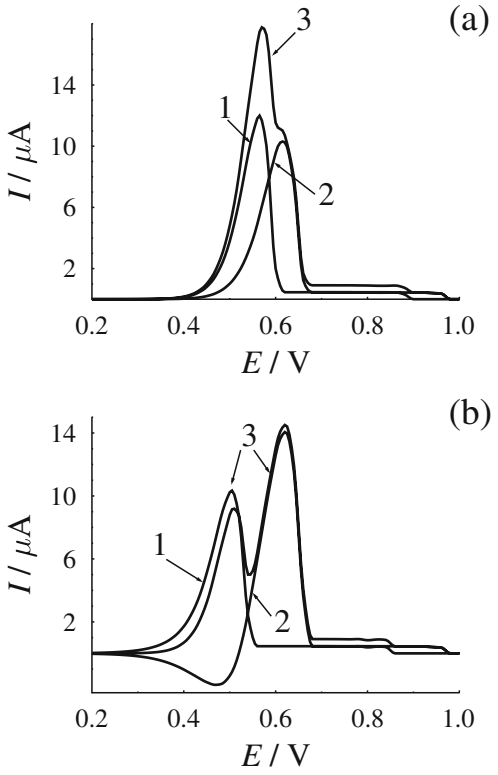


**Fig. 9** Voltammograms calculated for particles of similar size: $r_{0III}=5$ nm, $r_{0II}=20$ nm, $k_s=10^{-4}$cm s$^{-1}$, $\Delta G°=0$ (**a**) and 5,000 J mol$^{-1}$ (**b**). (*1*) $I_{III}$, (*2*) $I_{II}$, (*3*) $I_{III}+I_{II}$. Other parameters are given in the Fig. 3 caption

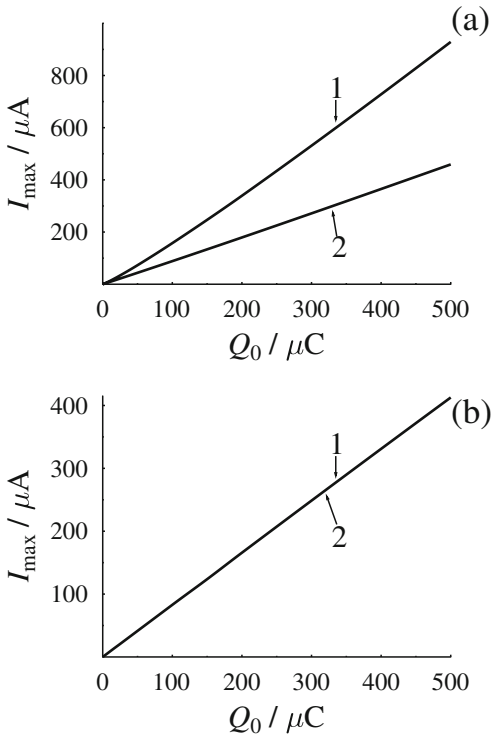


**Fig. 10** Maximal currents $I_{II}$ and $I_{III}$ dependence on the corresponding values of $Q_0$: $\Delta G°=1{,}000$ J mol$^{-1}$, $r_{0\,III}=5$ nm, $k_s=10^{-4}$ (**a**) and $10^{-7}$cm s$^{-1}$ (**b**)

**Table 1** Values d$I$/d$Q$ for reversible and irreversible processes (various $k_s$)

| $k_s$ | $dI_{III}/dQ_{III}$ $r_{0\ III}$=5nm | $dI_{II}/dQ_{II}$ |
|---|---|---|
| $10^{-4}$ reversible process | 1.22 | 0.87 |
| $10^{-7}$ irreversible process | 0.84 | 0.84 |

practically are overlapped, forming one peak I. At $\Delta G°$= 5,000 J mol$^{-1}$, we see partly overlapped distinguished peaks. In addition, a very interesting fact is observed: the increase of current $I_{III}$ is followed by appearance of negative (cathodic) current, corresponding to $I_{II}$. It is obviously the consequence of appearance of metal ions in near-electrode layer as a result of dissolution of small nanoparticles.

The new results (Figs. 1, 3, 4, 5, 6, 7, 8, and 9) and the published data (Fig. 2) thus confirm the aforementioned view that decrease in the surface energy and increase in the particle radius result in the system properties becoming closer to the properties of the corresponding bulk phase, i.e., a decrease in the metal contribution to the $M_{III}$ state and increase in the metal contribution to the state $M_{II}$ to the system properties. This conclusion is obvious both from the general views and stems also from the conditions 2 and 3 of the problem.

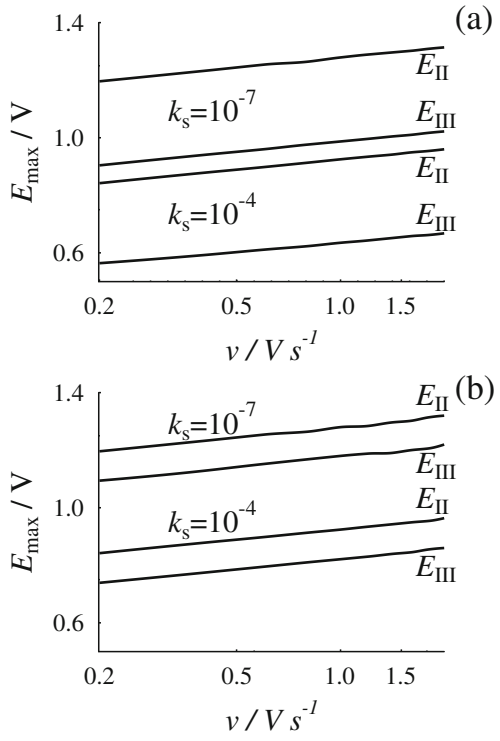


**Fig. 11** Maximal current potential dependence on the potential sweep rate: $\Delta G°$=1,000 J mol$^{-1}$, $Q_0$=20 μC, $r_{0\ III}$=5 (**a**) and 200 nm (**b**), $r_{0\ II}$=1 μm

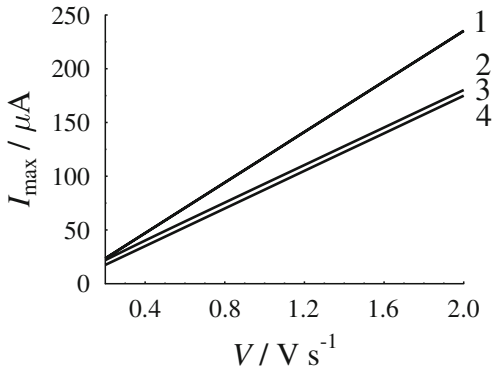


**Fig. 12** Current maximum dependence on the electrode potential sweep rate: $\Delta G°$=1,000 J mol$^{-1}$, $Q_0$=20 μC, $r_{0\ III}$=5 nm, $r_{0\ II}$=1 μm, $v$=0.20 V s$^{-1}$, $\delta$=0.50, 1,3-$I_{III}$, 2,4-$I_{II}$, $k_s$=10$^{-4}$ (1,2) and $k_s$=10$^{-7}$ (3,4)

Thus, assigning the values for $\Delta G°$ and the size of the studied particles calculated by, Eq. 14, we can predict the shape of the voltammograms, and, conversely after obtaining an experimental series of voltammograms for varying sizes of particles, we can estimate the Gibbs energy of the studied system and assess the critical particle radius, i.e., the radius at which the metal acquires the properties of the bulk metal.

Figure 10 shows the dependences of the maximum currents $I_{III}$ and $I_{II}$ on the corresponding values $Q_0$. It is apparent that, in the irreversible process, currents $I_{II}$ and $I_{III}$ essentially do not differ in magnitude. In the reversible process, current $I_{III}>I_{II}$. Table 1 shows the corresponding d$I$/d$Q$ values.

Figure 11 shows the dependences of the maximum current potentials on potential sweep rate (logarithmic scale). $\Delta E/\Delta(\log v)$=0.18 regardless of $k_s$ and $r$.

Figure 12 shows the dependence of the current maximum on the electrode potential sweep rate. It is apparent from the cited data that, in the irreversible process, currents $I_{II}$ and $I_{III}$ essentially do not differ from each other (at $Q_{II}$= $Q_{III}$). In the reversible process, current $I_{III}>I_{II}$.

## Conclusion

Size-dependent property is one of the essential features of nanostructured materials that should be taken into account in consideration of their electrochemical behavior. Of great significance is a study by *Krebbs* and *Roe* [15] who investigated discharge ionization of silver on single-silver crystals. They found a higher reactivity of a fresh metal deposit compared to a bulk metal. They observed an extremely interesting fact: clearly pronounced peak of dissolution of this deposit from the surface of the like electrode. This phenomenon can be considered as prognostication of nanoparticle behavior. Our preliminary experi-

ments have demonstrated appearance of metal nanoparticles electrooxidation peak on voltammogram at the less-positive potential, then bulk metal electrooxidation peak.

In previous works, microparticles or nanoparticles are considered as independent electrodes, and electroactive substance diffuses to its surface from the solution. In these cases, process kinetics is determined by diffusion zone geometry (overlapping, for example). In our case, anodic process (electrodissolution) is considered. Electroactive substance is uniformly distributed nanoparticles localized on the electrode surface and electrode process products are taken off by diffusion. Namely, the concentration of this product in the near-electrode layer determines cathodic-stage kinetics in reversible process. The most publications concerning metal nanoparticles dissolution process modeling include the concentration field determination stage near a separate particle (kinetics approach analog). At that, the effect of one or another type of symmetry is taken into account (symmetry cell allocation, mutual-particle location specification, isotropy of particles dissolution near a surface postulate, etc.).

We proposed a new alternative approach to the nanoparticle electrodissolution consideration. We draw an analogy with the thermodynamic method where the ion concentration near the dissolving metal particles can be determined without the detailed analysis at the separate particle level and their location consideration. An electrode with the huge amount of nanoparticles on it is considered as a continuously acting plane source with its intensity current being measured in the course of experiment. The corresponding diffusion problem appears to be spatially one-dimensional and its solution can be found rather easily. Concentration expression in terms of current allows us to close the model and to obtain an equation concerning the current. It is considered that anodic stage takes place on nanoparticles (those are the product sources) that determine cathodic stage of the process kinetics. Thus, our model is notable for it is based on the thermodynamic approach and considers an energy factor, namely the contribution of the surface energy to the energy of the system which is extremely appreciable for the nanoparticles.

The above-mentioned approaches that are supplement with one another present different investigation methods of a complicated polyvalent process. However, in the absence of the knowledge of the process details, the thermodynamic approach seems to be the most preferable.

Taking into account previously published [10, 11, 15] data and known substantial contribution of surface energy into system energy, we introduced Gibbs energy into equations that serve for electrode process description. Thus, mathematical model proposed have given an opportunity to simulate nanoparticles electrooxidation and obtained a series of voltammograms corresponding to different parameters. It has been shown that with a specific surface tension a very pronounced dependence of the Gibbs surface energy on the particle radius appears, which agrees with the generally accepted ideas and the aforementioned dependence of metal melting point on the metal particle size. This indicates that the proposed method is substantiated for estimating the quantity $\Delta G^\circ$ that is used in the calculations. The shape of the calculation voltammograms (presence of one or two peaks), current distribution, and difference in current peak potentials are determined by the magnitude of Gibbs energy and the particle radius. A difference in the quantities $dI/dQ$ and $dE/d(\log v)$ is observed for currents $I_{III}$ and $I_{II}$. Mathematical modeling of electrooxidation of metal nanoparticles has thus shown an interrelationship between the size and surface energy effects and shapes of the experimental curves. This confirms that electrochemical methods may be used as the source of very valuable information both for analysis of thermodynamic and energy properties of nanomaterials and the kinetics of redox reactions of nanoparticles. In subsequent papers, we will demonstrate the agreement between theory and experiment and some possible practical applications of electrochemical information.

**Acknowledgements** The authors are very grateful to RFBR (projects 07-03-96070-p_ural_a and 07-03-96068-p_ural_a) for their financial support.

## References

1. Ward Jones SE, Compton RG (2008) Curr Anal Chem 4:177
2. Welch CM, Compton RG (2006) Anal Bioanal Chem 384:601
3. Dai X, Compton RG (2006) Anal Sci 22:567
4. Dai X, Compton RG (2005) Electroanalysis 17:1325
5. Pumera M, Sanchez S, Ichinose I, Tang J (2007) Sens Actuator B 123:1195
6. Huang X-J, Choi Y-K (2007) Sens Actuator B 122:659
7. Riu J, Maroto A, Rius FX (2006) Talanta 69:887
8. Sarah E, Jones W, Campbell FW, Baron R, Xiao L, Compton RG (2008) J Phys Chem 112:17820
9. Sarah E, Jones W, Zheng SH, Craig A, Seretis S, Sylvie Morin J, Compton RG (2008) J Electroanal Chem 616:38
10. Brainina K, Neyman E, Slepushkin V (1988) Electroanalytical stripping methods. Chemistry, Moscow
11. Brainina KH, Neyman E (1993) Electroanalytical stripping methods. Series of monographs on analytical chemistry and its applications, vol 126. Wiley, New York
12. Carslaw HS, Jaeger JC (1986) Conduction of heat in solids, 2nd edn. Oxford University Press, Oxford
13. Buzea C, Ivan I, Blandino P, Robbie K (2007) Biointerphases 4:17
14. Zachariah MR, Carrier MJ, Blaisten-Barojas E (1996) J Phys Chem 100:14856
15. Krebbs WM, Roe DK (1967) J Electrochem Soc 114:192